

Terrestrial hydrological controls on land surface phenology of African savannas and woodlands

Kaiyu Guan^{1,2 *}, Eric F. Wood¹, David Medvigy³, John Kimball^{4,5}, Ming Pan¹, Kelly K. Caylor¹, Justin Sheffield¹, Xiangtao Xu³ and Matthew O. Jones^{4,5}

¹ Department of Civil and Environmental Engineering, Princeton University, Princeton, NJ 08544

² Department of Environmental & Earth System Science, Stanford University, Stanford, CA 94025

³ Department of Geosciences, Princeton University, Princeton, NJ 08544

⁴ The University of Montana Flathead Lake Biological Station, Polson, MT 59860

⁵ Numerical Terradynamic Simulation Group, University of Montana, Missoula, MT 59812

* Corresponding author: Kaiyu Guan

Tel: +1-609-647-1368

Email: kaiyug@stanford.edu

Submitted to *Journal of Geophysical Research - Biogeosciences*

This article has been accepted for publication and undergone full peer review but has not been through the copyediting, typesetting, pagination and proofreading process which may lead to differences between this version and the Version of Record. Please cite this article as doi: 10.1002/2013JG002572

Abstract:

This paper presents a continental-scale phenological analysis of African savannas and woodlands. We apply an array of synergistic vegetation and hydrological data records from satellite remote sensing and model simulations to explore the influence of rainy season timing and duration on regional land surface phenology and ecosystem structure. We find that: (i) the rainy season onset precedes and is an effective predictor of the growing season onset in African grasslands. (ii) African woodlands generally have early green-up before rainy season onset, and have a variable delayed senescence period after the rainy season, with this delay correlated non-linearly with tree fraction. These woodland responses suggest their complex water use mechanisms (either from potential groundwater use by relatively deep roots or stem-water reserve) to maintain dry season activity. (iii) We empirically find that the rainy season length has strong non-linear impacts on tree fractional cover in the annual rainfall range from 600-1800 mm/year, which may lend some support to the previous modeling study that given the same amount of total rainfall, the tree fraction may first increase with the lengthening of rainy season until reaching an “optimal rainy season length”, after which tree fraction decreases with the further lengthening of rainy season. This non-linear response is resulted from compound mechanisms of hydrological cycle, fire and other factors. We conclude that African savannas and deciduous woodlands have distinctive responses in their phenology and ecosystem functioning to rainy season. Further research is needed to address interaction between groundwater and tropical woodland as well as to explicitly consider the ecological significance of rainy season length under climate change.

Key Words:

phenology, Africa, savanna, rainy season, growing season, NDVI, Vegetation Optical Depth (VOD), TRMM, GRACE

1. Introduction:

“Vegetation phenology” refers to the periodic biological lifecycle events of plants, such as leaf flushing and senescence, and corresponding temporal changes in vegetation canopy cover [Stöckli et al., 2011]. This concept is linked tightly with plant establishment, growth, and reproduction [Morissette et al., 2009; Scheiter and Higgins, 2009], and also connects to the biosphere-atmosphere fluxes of energy, water and carbon [Bonan, 2008]. Thus vegetation phenology has critical significance to ecosystem functioning and associated services. Global warming has advanced the biological spring and lengthened the Northern Hemisphere growing season [Zhou et al., 2001; Myneni et al., 1997], because temperature is a dominant trigger for vegetation phenology in temperate ecosystems [Nemani et al., 2003]. These changes have large impacts on the regional carbon budgets [Richardson et al., 2010; Piao et al., 2008] and may have complex feedbacks to climate [Richardson et al., 2013]. However, it remains less clear how climate change has altered and will alter vegetation phenology in water-limited ecosystems, and associated implications for carbon cycling and climate feedbacks. Future climate is expected to transform precipitation patterns in a complex way [Weltzin et al., 2003; Trenberth et al., 2003], with changes in the rainy season projected over various water-limited regions of the world. For example, shortening and a seasonal shift in the rainy season have been projected for the Sahel [Biasutti and Sobel, 2009] and Southern Africa [Shongwe et al., 2009], which imposes urgency for better understanding about how climate and surface hydrological processes control vegetation phenology in water-limited ecosystems. This urgency is exemplified in Africa, where dry/semi-dryland ecosystems cover more than 60% of the continental landmass, and large uncertainties remain in predicting ecosystem responses to rainfall regime shifts in concert with other climatic changes [Giannini et al., 2008; Higgins and Scheiter, 2012].

Empirically studying the relationship of climate and vegetation phenology requires the availability of reliable data at proper spatial scales. Satellite remote sensing provides relatively consistent measurements of a range of land surface phenology attributes across space and time, which makes it possible to analyze large-scale patterns of vegetation

phenology and its relationship with climate. Satellite remote sensing measures spatially integrated vegetation attributes over variable footprints ranging from approximately 100m to 25km; this landscape level metric is termed “Land Surface Phenology (LSP)” [Morisette et al. 2009]. It is worth noting that this definition differs from the traditional “vegetation phenology”, which is usually based on in situ observations of individual plants or species. LSP is a combined signal of phenological behaviors of many individual plants in a landscape, thus also contains landscape and structural information (e.g. fraction of tree/grass/bare soil). We define various phases of LSP from time series of remotely sensed vegetation indices (e.g. Figure 1a), which are used as proxies of regional vegetation growth, senescence and dormancy at the satellite pixel scale [Zhang et al., 2003]. Previous LSP studies over Africa have primarily involved analyzing optical and near-infrared (NIR) based spectral vegetation greenness indices, including the NDVI (Normalized Difference Vegetation Index) and EVI (Enhanced Vegetation Index); these studies include analyzing spatial gradients in phenological dates [Zhang et al., 2005; Camberlin et al., 2007]; phenological trajectory differences in different biomes and climate [Martiny et al., 2006; Guan et al., 2013]; temporal trends in phenological dates [Tateishi and Ebata, 2004; Linderman et al., 2005; Heumann et al., 2007; Vrieling et al., 2013]; attributions of phenology behavior to rainfall [Philippon et al., 2005], temperature and humidity [Brown et al., 2012], and large climate oscillations [Brown et al., 2010]. Studies explicitly assessing inter-annual variability between the rainy season and regional vegetation phenology are lacking, and very few studies have addressed the temporal advances or lags among different phases of the rainy season and growing season. Filling these gaps has become possible only recently as synergistic satellite data records for precipitation and vegetation have accumulated over more than a decade, attaining a minimum length for statistical analysis of inter-annual relationships.

Our previous study [Guan et al., 2013] demonstrated that African savannas and woodlands, unlike tropical evergreen forests, have clear phase correspondence between the rainy season and vegetation growing season, i.e. they are largely overlapping in time. However, this temporal correspondence is mostly driven by the strong impacts of dry season, during which

lack of moisture shuts down most plant physiological and metabolic activities in dryland and semi-dryland ecosystems. In addition, this first-order seasonal correspondence could not explain what specific environmental factors trigger canopy leaf-flushing and senescence, and what factors control inter-annual variability in these phenological properties. For example, early leaf-flushing in the African Miombo Woodlands has been widely observed before the arrival of seasonal rainfall [[Chidumayo, 1994](#); [Fuller and Prince, 1996](#); [Seghieri et al., 2012](#)], with delayed senescence in many woody species after the end of the rainy season [[Bie et al., 1998](#); [Seghieri et al., 1995](#)]. These unresolved phenological behaviors call for a more detailed study on the relationships between the rainy season and regional land surface phenology, including canopy growth onset and senescence.

Tropical savannas are mostly water-limited, and are characterized by the coexistence of grasses and trees [[Scholes and Archer, 1997](#)], which may have different life cycle strategies and phenological responses. Grasses (mostly C_4 in Africa) usually follow the “pulse-reserve” paradigm [[Noy-Meir, 1973](#)] and opportunistically use water resources whenever is available to support their growth; the phenological response of these grasslands is expected to closely track shallow soil moisture dynamics [[Scanlon et al., 2005](#)]. While woody vegetation species may initiate growth using stored carbon reserves acquired during the previous season [[Scheiter and Higgins, 2009](#)], they may also have the ability to access other water resources (e.g. groundwater or stem-water reserve) to sustain vegetation activity during the dry season [[Bie et al., 1998](#)] and develop more complex desiccation tolerance and desiccation resistance structures through deeper roots and stem water storage etc. [[Pineda-Garcia et al. 2013](#)]. These features may indicate a different and more complex phenological response beyond the “pulse-reserve” paradigm. The ecological niche separation of water resource use in both space (i.e. root depth [[Walter, 1931](#); [Ward et al., 2013](#)]) and time (i.e. phenology [[Higgins et al., 2011](#)]) may contribute to the tree-grass coexistence pattern in tropical savannas. Thus analyzing the heterogeneous phenological responses in conjunction with hydrological processes across large regional gradients in climate and biome distribution is critical for

developing better vegetation phenology mechanistic in vegetation dynamic models for water-limited ecosystems.

As the rainy season provides the temporal niche for favorable vegetation growth conditions in African dryland and semi-dryland ecosystems, it is also important to understand how the length of rainy season impacts ecosystem productivity or structure. Highly seasonal rainfall can reduce the rate of canopy closure [[Schimper, 1903](#); [Sarmiento et al., 1984](#)] and facilitate grass expansion [[Lloyd et al., 2008](#)], and can increase fire frequency [[Archibald et al., 2009](#); [Lehmann et al., 2011](#); [Starver et al., 2012](#)]. In particular, from the hydrological perspective, the same amount of rainfall occurring over different time spans can have variable impacts on the partitioning of the terrestrial water budget (e.g. transpiration, evaporation, runoff) and influence vegetation growth, and rainy season length may explain regional patterns in vegetation phenology and tree cover. An important question is whether tree fractional cover increases monotonically with longer rainy season. Recent modeling studies [[Feng et al., 2012](#); [Rohr et al., 2013](#)] have found that rainy season length has a nonlinear impact on vegetation productivity from a hydrological perspective. This paper will present a possible empirical evidence for this theory.

This paper empirically studies relationships between rainy season and LSP seasonal phases and inter-annual variability across African savanna and woodland ecosystems. We examine spatial and temporal relations between rainy season length and vegetation onset and senescence periods, and associated impacts on vegetation structure (i.e. tree fraction), by employing multiple synergistic satellite derived vegetation and hydrological data records, and hydrological model simulations for the period from 2000-2010. This investigation is motivated by the following questions: 1) How does the timing of the rainy season (i.e. onset/offset) influence land surface phenology of woodlands and open savannas in Africa, including LSP seasonal and inter-annual variability? 2) How do variations in rainy season length influence proportional tree cover and associated ecosystem structure across the region? The paper first introduces the datasets and LSP-extraction methods used for the analysis

(Section 2), and then presents pixel-level time series of remotely sensed vegetation status and hydrological variables for selected representative pixels over the study area (Section 3.1). We then focus on analyzing continental scale relationships between the start (end) of the rainy season and start (end) of the growing season in Sections 3.2 and 3.3, respectively. Section 3.4 presents an empirical pattern related to the non-linear impacts of rainy season length on fractional tree cover, followed by general discussion and conclusions on the significance of these results.

2. Materials and Methods

This study focuses on understanding the relationship between land surface phenology and the rainy season for vegetated regions of Africa between 20°N and 30°S that display a unimodal growing season. In this domain, water availability has a dominant influence on vegetation dynamics [Nemani et al., 2003; Guan et al., 2014]. Land cover within the study domain is dominated by tropical deciduous woodlands (also referring as “woodlands” in this study) and tropical open savanna (also referring as “savannas” hereafter. See Figure 1b), with some cropland areas mainly clustered in the Sahel region. The major differences between “tropical deciduous woodlands” and “tropical open savannas” are whether there is a closure of tree canopy in the landscape (Lehmann et al., 2011). In this study, we group African cropland areas into the “tropical open savannas”. Physiologically most Africa crops are C₄ plants, most African croplands are fragmented and mixed with natural savannas, and there is very little irrigated agriculture in the region, so we can assume that croplands and grasslands would have similar phenology patterns. Other African vegetated regions (north of 20°N or south of 30°S) are excluded in this study because these areas reflect Mediterranean climate conditions, with relatively dry summers and rainy winters, and where both temperature and water supply can influence vegetation phenology [Peel et al., 2007]. We distinguished between regions with single or multiple growing seasons using Fourier power spectra, following Guan et al. [2014].

2.1 Dataset

2.1.1 Normalized Difference Vegetation Index (NDVI)

We used the daily NDVI calculated from red (620-670 nm) and near-infrared (841-876 nm) spectral reflectance bands of the Moderate Resolution Imaging Spectroradiometer (MODIS) MOD09CMG product (Collection 5, level 3) [Vermote et al., 2011]. This global dataset has been corrected to reduce the effects of atmospheric gases and aerosols. Only best possible data retrievals (i.e. Quality Control flag of the first two bits is 00 or 01) are used in the study. The original 0.05° spatial resolution of the MOD09CMG product was aggregated to 0.1° in this study. The daily temporal resolution is the primary reason for choosing this dataset over other MODIS vegetation index products available at coarser 8-16 day temporal resolution. The MODIS record for years 2000 to 2011 is used in this study. Due to the noisy conditions of the daily NDVI dataset, a fitting preprocessing to recover the envelope of the time series [Chen et al., 2006] was used before implementing the phenological extraction algorithm.

2.1.2 Microwave Vegetation Optical Depth (VOD)

We used a satellite passive microwave remote sensing based VOD product [Jones et al., 2010; Jones et al., 2011] from the Advanced Microwave Scanning Radiometer for EOS (AMSR-E), to assess phenological changes in vegetation canopy biomass structure [Guan et al., 2012]. The VOD parameter is a frequency dependent measure of canopy attenuation of microwave emissions, which represents changes in vegetation biomass and water content [Ulaby et al., 1982; Jones et al., 2013]. The VOD record has been used as an additional canopy phenology measure that is sensitive to both photosynthetic and non-photosynthetic (e.g. woody) biomass [Jones et al., 2011; Guan et al., 2012], whereas the MODIS NDVI record primarily detects changes in canopy-top photosynthetic vigor or potentials. We used the near-daily 10.7 GHz frequency VOD retrievals at the constant incidence angle of 55° from nadir from an existing AMSR-E global land parameter database for ecosystem studies [Jones and Kimball, 2010]. A detailed description of the AMSR-E VOD record, including algorithm development and sensitivity, can be found in Jones et al. [2010, 2011]. In this study, we used the daily VOD record from 2003 to 2011, and a robust smoothing algorithm [Garcia, 2010] was applied to

gap-fill missing values and smooth the daily time series. The original 0.25° spatial resolution was interpolated to 0.1° for the analysis.

2.1.3 Tree fractional cover data

In this study we use satellite derived tree fractional cover as a metric of ecosystem structure pertaining to the relative abundance of woody vegetation cover. We used a tree fractional cover dataset based on the algorithm of Guan et al. [2012] by combining satellite active microwave data (Ku-band backscattering coefficient from QuikSCAT [Long, 2001]) and passive optical-NIR reflectance data (MODIS EVI [Solano et al., 2010]). This product represents an integration of optical-NIR and active microwave remote sensing based on the mean vegetation state and inter-annual vegetation sensitivity to precipitation. This product outperformed the MODIS VCF product [Hansen et al., 2003] when compared with tree fractions derived from high-resolution imagery for natural vegetation [Guan et al., 2012]. However, our analysis indicates that use of the tree fractional cover data or MODIS VCF data (not shown) generate similar relationships between tree cover and rainy season length (Section 3.4); thus the relevant finding is independent of the tree fractional cover data that is used.

2.1.4 TMPA precipitation data

We used gridded precipitation data from the version 3B42V6 Tropical Rainfall Measurement Mission (TRMM) Multi-satellite Precipitation Analysis (TMPA) [Huffman et al., 2007]. The TMPA 3B42V6 is a 3 hourly, 0.25° product based on multi-satellite retrievals that combine microwave and infrared remote sensing estimates, and are rescaled to match monthly gauge observations using histogram matching [Huffman et al., 2007]. The TMPA product was converted from its original 0.25° and 3 hourly resolution to a 0.1° and daily resolution for the 2000-2011 data record for this study.

2.1.5 VIC-simulated soil moisture

Measurements of large-scale soil moisture are only available from satellite microwave-based soil moisture products either derived from remotely-sensed brightness temperatures from passive radiometries [Jackson, 1993] or active backscattering from scatterometers [Wagner et al., 1999]. However, these soil moisture retrievals are only sensitive to water content shallower than approximately 3cm in the top layer of the soil column, while the soil moisture signal is degraded under higher vegetation biomass levels [Njoku and Entekhabi, 1996]; this limits capabilities for studying soil hydrology and vegetation dynamics given that most vegetation (esp. trees) in Africa can be sensitive to much deeper soil moisture levels [Do et al., 2005, 2008; Seghieri et al., 2012]. Here we used simulated soil moisture from a macro-scale hydrological model, Variable Infiltration Capacity (VIC) [Liang et al., 1994]. The VIC model simulates sub-daily terrestrial water and energy balances and represents sub-grid variability in soil water storage capacity as a spatial probability distribution [Liang et al. 1994]. The VIC model has been applied extensively at regional (e.g. [Maurer et al. 2002]) and global scales (e.g. [Nijssen et al. 2001; Sheffield and Wood, 2007]). The VIC model was used in this study to generate the retrospective soil moisture profile at two soil depths: 0-10 cm and 10 cm-1 meter. The TMPA rainfall record (interchangeable with “TRMM rainfall” hereafter in this paper) [Pan et al. 2010] and other climate variables from the Global Meteorological Forcing Dataset (GMFD) of Princeton University [Sheffield et al., 2006] were used to force the VIC model for the period from 2000-2010 running at 0.25 degree resolution and 3 hourly time step [Pan et al. 2012], with calibrated model parameters from Sheffield and Wood [2007], which further refined the coarse soil texture and hydrology-related properties at local scales. The soil moisture output was interpolated to 0.1 degree resolution and daily time step for the analysis. It is worth noting that the VIC model-simulated soil moisture is only used here for diagnostic analysis rather than prognostic purposes.

2.1.6 GRACE terrestrial water storage

The terrestrial water storage variations captured by the Gravity Recovery and Climate Experiment (GRACE) satellite were used to study the potential interactions between subsurface water storage changes and land surface phenology. The GRACE satellite measures the total change in the terrestrial water storage (including surface and ground water elements, and water stored in vegetation) through associated changes in the Earth's gravity field [Rodell and Famiglietti, 2002; Tapley et al., 2004]. The terrestrial water storage from the GRACE is found to be highly correlated with the changes in soil moisture and groundwater in various ecosystems [Strassberg et al., 2009; Pokhrel et al., 2013]. Vegetation biomass signals are one to two orders of magnitude smaller than atmospheric and other terrestrial influences, and have little contribution to overall changes in the GRACE gravity field [Rodell et al., 2005]. Thus the GRACE terrestrial water storage retrieval can be safely interpreted as an independent measure of subsurface water storage changes. We used the GRACE monthly land water mass grids (TELLUS_LAND_NC_RL05) global data record from Jet Propulsion Laboratory [Swenson and Wahr, 2006], which has a monthly time step and 1 degree spatial resolution, and has been processed using a 200 km radius Gaussian filter. The resulting GRACE data record from 2002 to 2011 is used in the current study.

2.2 Extraction of vegetation phenological information

We used a newly derived algorithm [Guan et al., 2014] to extract LSP information from the daily MODIS (MOD09CMG) NDVI record. This new algorithm fits a double-logistic curve to a daily input time series, which is similar to the MODIS phenological algorithm [Zhang et al., 2003], but with a more rigorous mathematical derivation and better boundary constraints. The algorithm provides all the necessary information to reconstruct the whole trajectory of a daily time series, and thus can provide more user-defined phenological timing criteria. In this study, we extracted the 10%, 20%, 50% and 90% thresholds of the seasonal range for both green-up and senescence periods (Figure 1a). We define the period when NDVI is above 90% of its range as the “maturity period”, and n%UP refers to the time when NDVI reaches n% of the seasonal range for the “green-up period”, which includes the whole period of the

increasing phase in NDVI trajectory; m%OFF refers to the time when NDVI drops to m% of the range from the peak value in the “senescence period”, which refers to the entire descending period of the NDVI trajectory. Using multiple phenological thresholds provides a more complete depiction of land surface phenology and also provides a way to quantify uncertainties in interpreting phenological information extracted from coarse-/medium-resolution remote sensing, given that there is still a lack of understanding regarding relationships between satellite-derived LSP observations and finer scale ground truth information [White et al., 2009, Jones et al. 2013].

2.3 Extraction of rainy season timing information

There is no consensus on the definition of the rainy season and its onset and end time [Marengo et al., 2001; Wang and LinHo, 2002]. Here we define rainy season starts at the time that the cumulative rainfall reaches a certain climatological percentile of mean annual precipitation (so called “Percentage” approach) in a “hydrological year” using gridded daily rainfall data on a per pixel basis. The “hydrological year” starts in the middle of the dry season, followed by the rainy season, and ends in the subsequent dry season; this definition applies to regions with only a single annual rainy season. The “hydrological year” is determined as follows: the TRMM multi-year mean daily rainfall data was temporally smoothed with a lengthening smoothing window size until there were only two inflection points for the first-order derivative of the smoothed time series corresponding to midpoints of the wet and dry seasons. Once determined, the “hydrological year” was fixed thereafter for each year. We then applied the definitions for onset and end of rainy season to each “hydrological year” on a per pixel basis. The rainy season onset date is defined when the cumulative rainfall of the selected year reaches a climatological threshold of 5% (or 10%) of the mean total annual rainfall; the rainy season end date occurs when the total rainfall from that date to the end of the “hydrological year” reaches a climatological threshold of 5% (or 10%) of annual rainfall. The use of the climatological percentile is convenient to apply to the entire study area, which spans a large annual rainfall gradient.

It is worth noting that there are other definitions of rainy season. For example, the AGRHYMET [1996] (also in [Brown et al., 2008]) defines the rainy season onset as the first day that the subsequent 10 days have at least 25mm of total rainfall, followed by another 20 days with at least 20 mm of total rainfall; if the second condition is not fulfilled, testing for the next day is resumed. We checked differences between the AGRHYMET approach and the Percentage approach (Figure S1), and found that both yield similar spatial patterns over Africa and the absolute differences are very small that they do not change the resulting patterns and the conclusion.

3. Results

3.1. Seasonal patterns of hydrological and phenological variables at pixel scale

The four-year time series (2003-2006) of hydrological variables (TRMM precipitation, VIC two layer soil moisture, GRACE water storage changes) and vegetation status from the satellite NDVI and VOD series from eight representative pixels across the study domain are presented in Figure 2, while the locations of the pixels are shown in Figure 3c. The following major findings are summarized in Figure 2:

(1) The seasonal VOD and NDVI trajectories are tightly coupled for grassland (e.g. Figure 2a and 2h); these two trajectories deviate in woodland areas, and the temporal disparity between VOD and NDVI increases with tree fraction ([Jones et al., 2012](#)), with VOD exhibiting relatively slower increase at the beginning of the growing season and delayed peak time. This pattern is consistent with the physical basis of these observations and with previous studies: NDVI is related to canopy photosynthetic activity [[Sellers et al., 1992](#); [Guan et al., 2012](#)], which generally responds quickly to environmental changes as demonstrated by a relatively rapid NDVI increase at the beginning of the growing season. For the plants with low biomass ($LAI < 3.5$), NDVI is highly correlated with LAI or vegetation aboveground biomass. In contrast, the VOD is sensitive to canopy-volume biomass and water content, including photosynthetic and non-photosynthetic (e.g. woody) canopy biomass components, and exhibits a slower characteristic seasonal response than the NDVI [[Jones et al., 2012](#)]. The late

peak of VOD indicates that regional plant biomass generally reaches its seasonal peak at the end of the rainy season. Thus in grassland, VOD and NDVI are closely tracking each other because the biomass and photosynthesis rates co-develop and have almost linear correlation under its low biomass volume; however, the large disparity between VOD and NDVI in woodland indicate the lags of biomass accumulation after the photosynthesis rhythm in tree-dominated landscape, which usually contains much larger plant biomass.

(2) Though the NDVI co-varies with rainfall seasonality in general, the initial seasonal increase in NDVI may precede the rainy season onset (e.g. in woodlands, Figure 2c and 2e) or lag behind it (e.g. in open savannas, Figure 2a and 2g). NDVI also persists for various amount of time following the end of the rainy season before reaches to full senescence (indicated as NDVI90%OFF) as shown in all the representative pixels in Figure 2. These patterns indicate that the rainy season alone may not fully explain African woodland phenology, while other terrestrial hydrological processes, propagated from rainfall, may play a significant role in explaining temporal offsets between the vegetation growing season and rainy season in different biomes.

(3) For the hydrological variables, seasonal phase differences are evident between precipitation, 1st and 2nd-layer soil moisture, and subsurface water storage anomalies (Figure 2). The 1st-layer soil moisture sharply increases following the rainy season onset (indicated by the dashed black line), and also quickly decays after the end of the rainy season. The deeper 2nd-layer soil moisture seasonality lags behind the shallower 1st-layer and has a slower decline following the end of the rainy season. Seasonal changes in regional subsurface water storage (including both soil moisture and groundwater) from GRACE show the largest phase lags with precipitation, especially in woodland areas. Here we interpret the period of increasing terrestrial water storage (TWS) from GRACE as the “recharging phase”, which indicates that water storage is replenished from rainfall inputs; similarly, decreasing TWS from GRACE indicates a “releasing phase” where water storage is being withdrawn. We find that the “releasing phase” in most woodland areas generally persists into the dry season when

the estimated 1st-/2nd-layer of soil moisture has been depleted (i.e. soil moisture in these layers reaches a seasonal minimum), possibly indicating that water storage deeper than 1 meter may be being steadily withdrawn during the remainder of the dry season.

3.2. Start of rainy season and growing season at the continental scale

The relationships between the regional rainy season and growing season onset are described below. The spatial patterns of rainy season and growing season onset averaged over the 2000 to 2010 record are presented in Figure 3. These results are summarized separately for northern-hemisphere Africa and southern-hemisphere Africa because the rainfall seasonalities of these two regions are reversed and are also controlled by different climate systems [Nicholson, 1996].

We find that the onset dates of both TRMM-derived rainy season and NDVI-derived growing season show similar spatial gradients for both southern and northern-hemisphere Africa. The northern-hemisphere Africa shows clear latitudinal correspondence in these two onset dates ($R^2=0.53$, $p<0.05$, Figure 3d), however the southern-hemisphere Africa has much lower correlation in space ($R^2=0.17$, $p=0.12$, Figure 3e), which is consistent with the finding of Zhang et al. [2005] based on two year MODIS phenological product. The major reason for the southern-northern difference is that the northern-hemisphere Africa has one dominate weather system (i.e Intertropical Convergence Zone, ITCZ [[Giannini et al., 2008](#)]), while the southern-hemisphere Africa has more complex weather system (including east–west-oriented component of the African ITCZ originated from the northern inland and the Indian Ocean and the westerly current which originates over the South Atlantic [[McHugh and Rogers, 2001](#); Nicholson, 1996; Cook, 2009]), which makes spatial pattern of the rainfall onset/end more complex.

One common feature for northern and southern Africa is that there are a significant number of pixels showing early NDVI green-up before rainy season onset, and this pattern does not change when using different thresholds for defining the growing season (NDVI 10%UP,

NDVI 20%UP) and rainy season metrics (TRMM 5%cumulative, TRMM 10% cumulative; see Figure S2). This pattern is evident in the southern Africa, as two distinct relationship regimes are apparent between NDVI growing season and TRMM precipitation onset (Figure 3e), with one regime clustering largely below the 1:1 line (blue dashed polygon in Figure 3e), where growing season onset generally occurs before the start of the rainy season. These two regimes are coincident with regional distribution of woodlands and open savannas (Figure 1b). For the whole African study area, the early-green-up regions encompass approximately 32% of the study domain (Figure 3c), and largely overlap with woodlands (e.g. Figures 1b and 7d). The difference between the onsets of rainy season and growing season is inversely correlated with tree fraction (Figure 7d, $R^2 = 0.73$, $p < 0.0001$), indicating that ecosystem structure can explain most spatial variance in vegetation phenology. These results confirm numerous other studies that have found many savanna tree species to green-up before the onset of the rains [[Borchert, 1994](#); [Fuller and Prince, 1996](#); [Do et al., 2005](#); [Higgins et al., 2011](#); [Seghieri et al., 2012](#)].

Two major mechanisms can possibly explain this early green-up in woodlands. One is the access to the groundwater through deep root systems found in many tropical deciduous trees [[Schenk and Jackson, 2002](#); [Roupsard et al., 1999](#)], and the other is the stem-water reserve that stored in tree trunks or roots [[Borchert, 1994](#)] to support dry-season green-up. Though in this study we do not have any field data to support the second mechanism, the GRACE data provides some possible evidence for the first mechanism. The GRACE TWS changes (Figure 2c and 2e) indicate that subsurface water is still being withdrawn in the dry season when simulated shallow soil moisture has been depleted (i.e. there would be very little soil evaporation). The phase differences between GRACE data and simulated shallow soil moisture may support that some tropical deciduous trees can use deeper groundwater resources to sustain dry-season vegetation activity.

We also study the inter-annual variability of onset dates for rainy season and growing season. We find that woodlands generally have much smaller inter-annual variability than grasslands

for both onset dates (Figure 4a and 4b; also Figure S3 and S4). Since the majority of woodlands have green-up before the onsets of rainy season, we expect that only open savannas may show some power of using rainy season onsets to predict growing season onsets. It turns out that only open savannas southern Africa have high correlations (Figure 4 and Figure S6), with a weaker and more dispersed correlation pattern in northern Africa, mostly due to the low inter-annual variability of rainy season onsets in the northern Africa (Figure 4b). Since rainy season onset does not cue on the start of the growing season (e.g. leaf-flushing) in woodlands, other environmental cues may trigger leaf-flushing of woodlands, such as photoperiod, insolation, or vapor pressure deficit [Do et al., 2005; Seghieri et al., 2012].

3.3. End of rainy season and growing season at the continental scale

We now focus on the end of the growing season and its associated environmental control. The regional satellite observations indicate that NDVI senescence has temporal lags of various lengths after the end of rainy season (Section 3.1). Across the whole Africa, the end of seasonal canopy maturity (i.e. NDVI 10% OFF and estimated start of senescence, Figure 5a) generally coincides with the timing of the VOD peak (indicating the timing of maximum canopy biomass, Figure 5d), while both of these metrics coincide with the end of the rainy season estimated from the TRMM (Figure 5c). However, the end of the vegetation senescence period (i.e. NDVI 90% OFF, Figure 5b) largely lags behind the end of the rainy season. These results are also consistent with the pixel level patterns in Figure 2.

We further quantify the NDVI senescence lag length by calculating the temporal difference between NDVI 90% OFF and the end of the rainy season, as shown in Figure 6. Figure 6b indicates that when tree fractional cover is below 0.5, the senescence lag time increases with greater tree fractional cover. In contrast, when the tree fraction is larger than 0.5, the senescence lag time decreases with increasing tree fractional cover. The positive correspondence between senescence lag and tree cover when tree fraction is below 0.5 may indicate a greater extent of deep rooted trees capable of either accessing deeper groundwater

resources or have stem-water reserve that enable a longer period of plant activity after the rainy season ends and surface soil moisture is depleted. However, this correlation pattern does not hold when tree fraction is above 0.5, which is mostly correspondent to the transitional regions from deciduous woodlands to evergreen forests. In these regions, rainy season lengths are significantly longer than the neighboring regions (Figure 7a), but growing season lengths remain similar with other woodlands as they are reaching saturation (with upper bound of 365 days, Figure 7b). In other words, in these regions, keeping lengthening rainy season does not further increase tree fraction cover as the latter reaches saturation. This explains why there is a weak decreasing trend in Figure 6b when tree fraction is above 0.5.

We also studied the temporal correspondence between the end of rainy season and other growing season phases. The end of the rainy season was poorly correlated with both the end of canopy maturity (NDVI10%OFF) and the end of canopy senescence (NDVI90%OFF) (results not shown). The low correspondence is primarily attributed to low inter-annual variability in both the rainy season ending time (Figure S5) and vegetation senescence phases (Figure S4). The vegetation senescence period of African woodlands generally exhibits little inter-annual variation (Figure S4, s.t.d.<10days), which indicates that canopy senescence in tropical woodlands is not very responsive to rainy season. Instead, senescence in these areas may be controlled by photoperiod or insolation-related environmental cues that show almost no inter-annual variation [Yeang, 2007; Borchert et al., 2005].

3.4. Non-linear impacts of rainy season length on tree fraction cover

Previous studies indicate a positive linear relationship between growing season length and tree fractional cover over Africa ($r = 0.73$, $p < 0.05$ [Guan et al., 2014]). The results of the current study confirm this general relationship (Figure 7c and 7d). However, the linkage between rainy season length and tree fraction is not clear and has not been explicitly addressed in previous studies. We further find that tree fractional cover does not simply correlate with mean annual precipitation or rainy season length within the African domain (e.g. Figure 7). Instead, we find a non-linear response of tree fractional cover to mean annual

precipitation and rainy season length (Figure 8a), which confirms the previous modeling study by Feng et al. [2012] and Rohr et al. [2013] that are mostly based on the plant water use. Here we define rainy season length as the period encompassing 90% of the total annual rainfall climatology. For rainfall regimes below 600 mm/year and above 1800 mm/year, tree fractional cover is directly proportional to mean annual precipitation. However, for intermediate rainfall regimes (i.e. 600 mm/year to 1800 mm/year), tree fractional cover shows a non-linear response to rainy season length: for a fixed mean annual precipitation, tree fraction increases with rainy season length until reaching a maximum proportional cover, where the corresponding rainy season length is denoted as the rainy season “optimal length”; tree cover then decreases with further increase of rainy season (see the inset of Figure 8a).

The nonlinear impacts of rainy season length on tree fractional cover may originate from various reasons [Schimper, 1903; Lloyd et al., 2008; Lehmann et al., 2011; Staver et al., 2012]. As Feng et al. [2012] and Rohr et al. [2013] have found from a hydrological perspective, given the same amount of total annual rainfall, the length of rainy season (and inversely the length of dry season) can influence water budget partitioning and rainfall use efficiency (defined as the percentage of rainfall ended up for plant growth through transpiration) [Huxman et al., 2004], and can impact vegetation dynamics. As rainy season increases from very short to longer period, less runoff would be expected and more rainfall would be used as transpiration and facilitate tree growth, and rainfall use efficiency would increase with the lengthening of the rainy season. However, when rainy season keeps increasing to be very long, more rainfall may be ended up as soil evaporation, and rainfall use efficiency would decrease. This hydrological mechanism, together with other factors, such as fire-mediated feedbacks [Staver et al., 2012], grazing pressure [van Schaik et al., 1993], and nutrient limitations [Fierer and Schimel, 2002], can influence the tree cover response to varying rainy season lengths. The observed pattern here, including the “optimal rainy season”, is a compounded consequence from all these possible factors, and fully attribute them is beyond the scope of this study. However, our result provides a possible evidence to support

the modeling study for the non-linear response of rainy season on vegetation productivity based on a hydrological mechanism.

Based on this pattern in Figure 8a, we calculate the empirical sensitivity of tree fraction with rainy season length under a fixed mean annual precipitation (i.e. the spatial gradient in Figure 8a in the y-axis direction), shown in Figure 8b. The blue and red colors in Figure 8b correspond to respective negative and positive tree fractional cover response to rainy season lengthening, and the white colors refer to the rainy season “optimal length” with a conceptual illustration in the inset of Figure 8a. These results show a general regional pattern of increasing “optimal length” with increasing mean annual precipitation. We also find that with the similar total rainfall amount (400-800 mm/year) but different rainy season lengths, northern African savannas (12°N-16°N) and southern African savannas (south of 22°S) show distinctive responses (Figure S7). From the hydrological perspective, northern African has a much shorter rainy season length and much more intense rainfall than regions in southern Africa (Figure S7). Thus northern African savannas, correspondent to the rectangular space in Figure 8, would benefit from increasing rainy season length as a means for distributing rainfall and supporting vegetation growth over a longer period; the increase in rainy season length would thus improve the rainfall use efficiency, and subsequently increase tree fractional cover. In contrast, southern African savannas, correspondent to the other identified regions in Figure 8, have a characteristically longer growing season length, where further increases in rainy season length coincide with reduced fractional tree cover.

We also find that most African woodlands show a positive sensitivity of tree fraction to increasing rainy season length, i.e. rainy seasons in these areas are generally below their “optimal length” and rainfall is not maximized for the growth of woody species. Thus, increasing rainy season length, i.e. to spread the same amount of total annual rainfall for a longer period, would promote an increase in tree fractional cover in these areas.

4. Discussion

4.1. Added value of VOD in studying savanna phenology

VOD represents the whole-canopy water content and biomass [Jones et al., 2012], and we find the inclusion of it with the more traditional NDVI metric from optical-NIR remote sensing improved the understanding of LSP dynamics for different vegetation properties in this study. Coupling VOD and NDVI illuminate distinctive phenology responses in grassland and woodland systems that may enable the separation of relative tree/grass contributions to the coarse-resolution remote sensing signal [Guan et al., 2012]. Further study of the VOD parameter, including use of variable microwave frequency retrievals in vegetation monitoring and modeling should be encouraged for characterizing vegetation aboveground biomass changes.

4.2. Dry-season water use mechanisms for explaining woodland phenology

Our results indicate that tropical woodlands generally green-up before the onset of rainy season and also keep active in the early dry season. It does not mean that early leaf-flush does not occur elsewhere (in the Acacias of the southern Kruger Park, for example), but it may only happen in a smaller fraction of total tree cover, and perhaps the duration of pre-rainfall leaf flush is less (e.g. Archibald and Scholes, 2007). The two major possible mechanisms include (1) access and use of subsurface water storage deeper than one meter by relatively deep rooted tropical deciduous trees, and (2) stem-water reserve stored in tree trunks and roots. Though in this study we could not fully answer which dominating mechanism function at a specific region due to the lack of stem-water measurements, we find some large-scale evidence to possibly support the first mechanism. When the simulated shallow-layer soil moisture (within one meter depth) is depleted during dry season, subsurface storage indicated from GRACE observations is still being withdrawn, which potentially can satisfy water needs for woody vegetation. This finding is consistent with some previous studies of tropical deciduous trees [Oliveira et al., 2005], which show that many tropical deciduous forests have deeply rooted and are capable of accessing deeper groundwater sources.

Regardless of which mechanisms, our results indicate that only using soil moisture thresholds as the phenological triggers in tropical deciduous forests (e.g. in LPJ [Sitch et al., 2003]; CLM [Levis et al., 2004]) may not be sufficient to characterize forest canopy phenology in these systems. Thus for tropical deciduous forests, explicitly incorporating a groundwater-vegetation interactive component or stem-water storage mechanism may be essential to correctly simulate vegetation dynamics in these ecosystems.

4.3. Prediction of grassland and woodland phenology from rainy season timing

Our results confirm the previous modeling study that rainy season timing strongly controls on grass-dominated savanna phenology. Our results also indicate that African woodlands have much less inter-annual variability in phenological timing than grasslands, and that their growing seasons can extend beyond the rainy season (i.e. early green-ups and delayed senescence). Though the rainy season overlaps with the growing season, it is not coincident with the onset and end of the growing season in African woodlands. The end of the rainy season appears to correspond with the end of canopy maturity (i.e. start of senescence) as indicated from the NDVI signal, and also with the timing of peak biomass indicated from the VOD signal. The potential factors controlling African woodland phenology is not obvious from our analysis. Radiation-related factors, e.g. photoperiod or insolation [Borchert et al., 2005; Yeang, 2007], or atmospheric water demands (vapor pressure deficit [Do et al., 2005; Seghieri et al., 2012]) have been proposed as possible triggers of canopy phenology in these regions, and some of these factors (e.g. photoperiod or insolation) have almost no inter-annual variability, which mirror the low inter-annual variability in tropical tree phenology. Further exploration on this topic is needed, especially field data related to both canopy phenology and hydrological variables in tropical deciduous forests.

4.4. Rainy season length and its ecological significance

Our result provides a possible empirical evidence to support the modeling study for the non-linear response of rainy season on vegetation productivity. It is worth noting that the emphasis of this possible hydrology-driven non-linear response does not devalue other

factors for savanna dynamics and tree fraction cover, but rather highlights some overlooked aspect that same rainfall but arrive in a different way may lead to diverse ecological responses. If we are convinced of the importance of rainy season length on ecosystem structure and function, we need to recognize that how well climate models predict future changes in rainy season length is also largely understudied, and the implications of these changes to future ecosystem productivity and biome distribution is also unknown. Thus it is imperative to include rainy season length and other rainy season characteristics in assessing the future eco-hydrological changes, especially in water-limited ecosystems.

4.5. Limitations of coarse-resolution remote sensing in studying savanna phenology

While there are many advantages in using relatively coarse spatial resolution (>100m) satellite remote sensing and hydrological modeling in studying African savanna phenology, a major drawback of these methods is the lack of resolution in differentiating the relative contributions of grasses and trees at the pixel level. This limitation hinders the interpretation of savanna phenology [Archibald and [Scholes, 2007](#)], e.g. whether the early green-up phenomenon is from grasses/shrubs or from trees, and the associated environmental cues driving these changes. Thus remote sensing at finer spatial resolutions is needed for resolving potentially contrasting grassland and woody vegetation dynamics in savanna ecosystems. Recent progress in unmanned aerial vehicle-based sensing systems (e.g. [[Dandois and Ellis, 2013](#)]) and the “near-surface remote sensing” (e.g. PhenoCam network [[Richardson et al., 2009](#)]) may provide possible avenues to resolve sub-grid scale heterogeneity in savanna ecology and phenology. Another possible avenue is to increase the coverage of ground observation networks to more effectively link remote sensing measurements with ground truth. Recently much progress has been made in developing relatively dense phenological observation networks in North America (e.g. USA National Phenology Network, USANPN) and Europe (e.g. European Phenology Network). A similar network is currently unavailable over Africa, but could provide an effective means for LSP validation and analysis, and improved understanding of regional phenology.

5. Conclusion

Understanding relationships between the hydrological cycle and land surface phenology in African savannas and woodlands has fundamental significance for modeling tropical vegetation dynamics, quantifying their carbon budget and predicting their future response to climate changes. This paper uses multiple datasets from satellite observations and hydrological model simulations to empirically explore temporal relationships between the hydrological cycle and regional phenology, and the nonlinear impact of rainy season length on ecosystem structure. The key findings from this study are summarized below:

- (i) We find that the annual growing season onset temporally lags and can be effectively predicted by the rainy season onset for African grasslands.
- (ii) Most African woodlands differ from grasslands and tend to have early green-up before the rainy season onset. African woodlands also show variable duration of senescence following the end of the rainy season, which has a non-linear correlation with tree fraction cover; inter-annual variability in woodland phenological phases is relatively small compared to African grasslands. We find some evidence to support the subsurface water use through deep root system (>1m depth) to maintain dry season vegetation activity.
- (iii) We empirically find the rainy season length has strong non-linear impacts on tree fractional cover in the annual rainfall range from 600-1800 mm/year, and there exists a rainy season “optimal length” for maximizing tree fractional cover at different rainfall regimes.

Acknowledgements:

K. Guan and E. F. Wood acknowledge the supports from the NASA NESSF fellowship and Walbridge Graduate Funds from Princeton Environmental Institute of Princeton University.

K. K. Caylor acknowledges the financial supports from the National Science Foundation through the Grant EAR-0847368. J. Kimball was supported through the NASA MEaSUREs (Making Earth System data records for Use in Research Environments) program.

Accepted Article

References:

AGRHYMET (1996), 'Méthodologie de suivi des zones à risque.', Technical report, AGRHYMET FLASH, Bulletin de Suivi de la Campagne Agricole au Sahel, Centre Regional AGRHYMET, Niamey, Niger.

[Archibald, S. & Scholes, R. \(2007\), 'Leaf green-up in a semi-arid African savanna—separating tree and grass responses to environmental cues', *Journal of Vegetation Science* **18**, 583-594.](#)

[Archibald, S.; Roy, D. P.; Van Wilgen, B. W. & Scholes, R. J. \(2009\), 'What limits fire? An examination of drivers of burnt area in Southern Africa', *Global Change Biology* **15**, 613-630.](#)

[Biasutti, M. & Sobel, A. H. \(2009\), 'Delayed Sahel rainfall and global seasonal cycle in a warmer climate', *Geophysical Research Letters* **36**, L23707.](#)

[Bie, S. D.; Ketner, P.; Paasse, M. & Geerling, C. \(1998\), 'Woody plant phenology in the West Africa savanna', *Journal of Biogeography* **25**, 883-900.](#)

Bonan, G. (2008), *Ecological Climatology: Concepts and Applications (2nd edition)*, Cambridge University Press, Cambridge, UK.

[Borchert, R. \(1994\), 'Soil and Stem Water Storage Determine Phenology and Distribution of Tropical Dry Forest Trees', *Ecology* **75\(5\)**, 1437-1449.](#)

[Borchert, R.; Renner, S. S.; Calle, Z.; Navarrete, D.; Tye, A.; Gautier, L.; Spichiger, R. & von Hildebrand, P. \(2005\), 'Photoperiodic induction of synchronous flowering near the Equator', *Nature* **433**, 627-629.](#)

[Brown, M.; de Beurs, K. & Marshall, M. \(2012\), 'Global phenological response to climate change in crop areas using satellite remote sensing of vegetation, humidity and temperature over 26 years', *Remote Sensing of Environment* **126**, 174-183.](#)

[Brown, M. E.; de Beurs, K. & Vrieling, A. \(2010\), 'The response of African land surface phenology to large scale climate oscillations', *Remote Sensing of Environment* **114\(10\)**, 2286-2296.](#)

[Camberlin, P.; Martiny, N.; Philippon, N. & Richard, Y. \(2007\), 'Determinants of the interannual relationships between remote sensed photosynthetic activity and rainfall in tropical Africa', *Remote Sensing of Environment* **106**, 199-216.](#)

[Chen, J. M.; Deng, F. & Chen, M. \(2006\), 'Locally Adjusted Cubic-Spline Capping for Reconstructing Seasonal Trajectories of a Satellite-Derived Surface Parameter', *IEEE Transactions on Geoscience and Remote Sensing* **44\(8\)**, 2230-2238.](#)

Chidumayo, E. N. (1994), 'Phenology and nutrition of miombo woodland trees in Zambia', *Trees* **9**, 67-72.

Dandois, J. P. & Ellis, E. C. (2013), 'High spatial resolution three-dimensional mapping of vegetation spectral dynamics using computer vision', *Remote Sensing of Environment* **136**, 259-276.

Do, F.; Rocheteau, A.; Diagne, A.; Goudiaby, V.; Granier, A. & Lhomme, J. (2008), 'Stable annual pattern of water use by *Acacia tortilis* in Sahelian Africa', *Tree Physiology* **28**, 95-104.

Do, F. C.; Goudiaby, V. A.; Gimenez, O.; Diagne, A. L.; Diouf, M.; Rocheteau, A. & Akpo, L. E. (2005), 'Environmental influence on canopy phenology in the dry tropics', *Forest Ecology and Management* **215**, 319-328.

Feng, X.; Vico, G. & Porporato, A. (2012), 'On the effects of seasonality on soil water balance and plant growth', *Water Resource Research* **48**, W05543.

Fierer, N. & Schimel, J. P. (2002), 'Effects of drying-rewetting frequency on soil carbon and nitrogen transformations', *Soil Biology & Biochemistry* **34**, 777-787.

Fuller, D. & Prince, S. (1996), 'Rainfall and foliar dynamics in tropical southern Africa: potential impacts of global climatic change on savanna vegetation', *Climatic Change* **33**, 69-96.

Garcia, D. (2010), 'Robust smoothing of gridded data in one and higher dimensions with missing values', *Computational Statistics and Data Analysis* **54**, 1167-1178.

Giannini, A.; Biasutti, M.; Held, I. M. & Sobel, A. H. (2008), 'A global perspective on African climate', *Climatic Change*, **90**, 359-383.

Good, S. P. & Caylor, K. K. (2011), 'Climatological determinants of woody cover in Africa', *Proceedings of the National Academy of Sciences of United States of America* **108(12)**, 4902-4907.

Guan, K.; Medvigy, D.; Wood, E. F.; Caylor, K. K.; Li, S. & Jeong, S.-J. (2014), 'Deriving vegetation phenological time and trajectory information over Africa using SEVIRI daily LAI', *IEEE Transactions on Geoscience and Remote Sensing* **53(2)**, 1113-1130.

Guan, K.; Wolf, A.; Medvigy, D.; Caylor, K.; Pan, M. & Wood, E. (2013), 'Seasonal coupling of canopy structure and function in African tropical forests and its environmental controls', *Ecosphere* **4(3):35**.

Guan, K.; Wood, E. F. & Caylor, K. K. (2012), 'Multi-sensor derivation of regional vegetation fractional cover in Africa', *Remote Sensing of Environment* **124**, 653-665.

Hansen, M. C.; DeFries, R. S.; Townshend, J. R. G.; Carroll, M.; Dimiceli, C. & Sohlberg, R. A. (2003), 'Global Percent Tree Cover at a Spatial Resolution of 500 Meters: First Results of the MODIS Vegetation Continuous Fields Algorithm', *Earth Interactions* **7**.

Heumann, B.; Seaquist, J.; Eklundh, L. & Jonsson, P. (2007), 'AVHRR derived phenological change in the Sahel and Soudan, Africa, 1982–2005', *Remote Sensing of Environment* **108**, 385-392.

Higgins, S. I.; Delgado-Cartay, M. D.; February, E. C. & Combrink, H. J. (2011), 'Is there a temporal niche separation in the leaf phenology of savanna trees and grasses?', *Journal of Biogeography* **38**, 2165-2175.

Higgins, S. I. & Scheiter, S. (2012), 'Atmospheric CO₂ forces abrupt vegetation shifts locally, but not globally', *Nature* **488**, 209-212.

Huffman, G. J.; Bolvin, D. T.; Nelkin, E. J.; Wolff, D. B.; Adler, R. F.; Bowman, K. P. & Stocker, E. F. (2007), 'The TRMM Multisatellite Precipitation Analysis (TMPA): Quasi-Global, Multiyear, Combined-Sensor Precipitation Estimates at Fine Scales', *Journal of Hydrometeorology* **8**, 38-55.

Huxman, T. E.; Smith, M. D.; Fay, P. A.; Knapp, A. K.; Shaw, M. R.; Loik, M. E.; Smith, S. D.; Tissue, D. T.; Zak, J. C.; Weltzin, J. F.; Pockman, W. T.; Sala, O. E.; Haddad, B. M.; Harte, J.; Koch, G. W.; Schwinning, S.; Small, E. E. & Williams, D. G. (2004), 'Convergence across biomes to a common rain-use efficiency', *Nature* **429**, 651-654.

Jackson, T. J. (1993), 'Measuring surface soil moisture using passive microwave remote sensing', *Hydrological Processes* **7**, 139-152.

Jones, L. A.; Ferguson, C. R.; Kimball, J. S.; Zhang, K.; Chan, S. K.; McDonald, K. C.; Njoku, E. G. & Wood, E. F. (2010), 'Daily land surface air temperature retrieval from AMSR-E: Comparison with AIRS/AMSU', *IEEE Journal of Selected Topics in Applied Earth Observations and Remote Sensing* **3(1)**, 111-123.

Jones, L. A. & Kimball, J. S. (2010), 'Daily Global Land Surface Parameters Derived from AMSR-E', Technical report, Boulder Colorado USA: National Snow and Ice Data Center. Digital media (<http://nsidc.org/data/nsidc-0451.html>).

Jones, M. O.; Jones, L. A.; Kimball, J. S. & McDonald, K. C. (2011), 'Satellite Passive Microwave Remote Sensing for Monitoring Global Land Surface Phenology', *Remote Sensing of Environment* **115(4)**, 1102-1114.

Jones, M. O.; Kimball, J. S. & Jones, L. A. (2013), 'Satellite Microwave Detection of Boreal Forest Recovery from the Extreme 2004 Wildfires in Alaska and Canada', *Global Change*

Biology **19**(10), 3111-3122.

[Jones, M. O.; Kimball, J. S.; Jones, L. A. & McDonald, K. C. \(2012\), 'Satellite passive microwave detection of North America start of season', *Remote Sensing of Environment* **123**, 324-333.](#)

[Jones, M. O.; Kimball, J. S.; Small, E. E. & Larson, K. M. \(2013\), 'Comparing land surface phenology derived from satellite and GPS network microwave remote sensing', *International Journal of Biometeorology*. doi: 10.1007/s00484-013-0726-z](#)

[Levis, S.; Bonan, G. B.; Vertenstein, M. & Oleson, K. W. \(2004\), 'The Community Land Model's Dynamic Global Vegetation Model. \(CLM-DGVM\): Technical Description and User's Guide', Technical report, NCAR.](#)

[Lehmann, C. E. R.; Archibald, S. A.; Hoffmann, W. A. & Bond, W. J. \(2011\), 'Deciphering the distribution of the savanna biome', *New Phytologist* **191**, 197-209.](#)

[Liang, X.; Lettenmaier, D. P.; Wood, E. F. & Burges, S. .. \(1994\), 'A simple hydrologically based model of land surface water and energy fluxes for general circulation models', *Journal of Geophysical Research* **99**, D7, 14,415-14,428.](#)

[Linderman, M.; Rowhani, P.; Benz, D.; Serneels, S. & Lambin, E. F. \(2005\), 'Land-cover change and vegetation dynamics across Africa', *Journal of Geophysical Research* **110**, D12104.](#)

[Lloyd, J.; Bird, M. I.; Vellen, L.; Miranda, A. C.; Veenendaal, E. M.; , G. D.; Miranda, H. S.; Cook, G. & Farquhar, G. D. \(2008\), 'Contributions of woody and herbaceous vegetation to tropical savanna ecosystem productivity: a quasi-global estimate', *Tree Physiology* **28**, 451-468.](#)

[Long, D. \(2001\), 'BYU Daily Browse Images of QuikSCAT Sigma-0 Measurements', Technical report, Brigham Young University.](#)

[Marengo, J. A.; Liebmann, B.; Kousky, V. E.; Filizola, N. P. & Wainer, I. C. \(2001\), 'Onset and End of the Rainy Season in the Brazilian Amazon Basin', *Journal of Climate* **14**, 833-852.](#)

[Martiny, N.; Camberlin, P.; Richard, Y. & Philippon, N. \(2006\), 'Compared regimes of NDVI and rainfall in semi-arid regions of Africa', *International Journal of Remote Sensing* **27**\(23\), 5201-5223.](#)

[Maurer, E. P.; Wood, A. W.; Adam, J. C.; Lettenmaier, D. P. & Nijssen, B. \(2002\), 'A Long-Term Hydrologically Based Dataset of Land Surface Fluxes and States for the Conterminous United States', *Journal of Climate* **15**, 3237-3251.](#)

Mayaux, P.; Bartholome, E.; Fritz, S. & Belward, A. (2004), 'A new land-cover map of Africa for the year 2000', *Journal of Biogeography* **31**, 861-877.

McHugh, M. J. & Rogers, J. C. (2001), 'North Atlantic Oscillation Influence on Precipitation Variability around the Southeast African Convergence Zone', *Journal of Climate* **14**, 3631-3642.

Morisette, J.; Richardson, A.; Knapp, A.; Fisher, J.; Graham, E.; Abatzoglou, J.; Wilson, B.; Breshears, D.; and J.M. Hanes, G. H. & Liang, L. (2009), 'Tracking the rhythm of the seasons in the face of global change: phenological research in the 21st century', *Frontiers in Ecology and the Environment* **7(5)**, 253-260.

Myneni, R. B.; Keeling, C. D.; Tucker, C. J.; Asrar, G. & Nemani, R. R. (1997), 'Increased plant growth in the northern high latitudes from 1981 to 1991', *Nature* **386**, 698 - 702.

Nemani, R. R.; Keeling, C. D.; Hashimoto, H.; Jolly, W. M.; Piper, S. C.; Tucker, C. J.; Myneni, R. B. & Running, S. W. (2003), 'Climate-Driven Increases in Global Terrestrial Net Primary Production from 1982 to 1999', *Science* **300**, 1560-1563.

Nicholson, S. E. Johnson, T. C. & Odada, E. O., ed., (1996), *The Limnology, Climatology and Paleoclimatology of the East African Lakes*, Gordon and Breach, New York, chapter A review of climate dynamics and climate variability in eastern Africa, pp. 25-56.

Nijssen, B.; Schnur, R. & Lettenmaier, D. P. (2001), 'Global Retrospective Estimation of Soil Moisture Using the Variable Infiltration Capacity Land Surface Model, 1980-93', *Journal of Climate* **14**, 1790-1808.

Njoku, E. G. & Entekhabi, D. (1996), 'Passive microwave remote sensing of soil moisture', *Journal of Hydrology* **184**, 101-129.

Noy-Meir, I. (1973), 'Desert Ecosystems: Environment and Producers', *Annual Review of Ecology and Systematics* **4**, 25-51.

Oliveira, R. S.; Bezerra, L.; Davidson, E. A.; Pinto, F.; Klink, C. A.; Nepstad, D. C. & Moreira, A. (2005), 'Deep root function in soil water dynamics in cerrado savannas of central Brazil', *Functional Ecology* **19**, 574-581.

Pan, M.; Li, H. & Wood, E. (2010), 'Assessing the skill of satellite-based precipitation estimates in hydrologic applications', *Water Resources Research* **46**, W09535.

Pan, M.; Sahoo, A. K.; Troy, T. J.; Vinukollu, R. K.; Sheffield, J. & Wood, E. F. (2012), 'Multisource Estimation of Long-Term Terrestrial Water Budget for Major Global River Basins', *Journal of Climate* **25**, 3191-3206.

Peel, M. C.; Finlayson, B. L. & McMahon, T. A. (2007), 'Updated world map of the Kuppen-Geiger climate classification', *Hydrology and Earth System Sciences* **11**, 1633-1644.

Philippon, N.; Mougin, E.; Jarlan, L. & Frison, P.-L. (2005), 'Analysis of the linkages between rainfall and land surface conditions in the West African monsoon through CMAP, ERS-WSC, and NOAA-AVHRR data', *Journal of Geophysical Research-Atmospheres* **110**, D24.

Piao, S.; Ciais, P.; Friedlingstein, P.; Peylin, P.; Reichstein, M.; Luysaert, S.; Margolis, H.; Fang, J.; Barr, A.; Chen, A.; Grelle, A.; Hollinger, D. Y.; Laurila, T.; Lindroth, A.; Richardson, A. D. & Vesala, T. (2008), 'Net carbon dioxide losses of northern ecosystems in response to autumn warming', *Nature* **451**(3), 49-53.

Pineda-Garcia, F.; Paz, H. & Meinzer, F. C. (2012), 'Drought resistance in early and late secondary successional species from a tropical dry forest: the interplay between xylem resistance to embolism, sapwood water storage and leaf shedding', *Plant Cell and Environment* **36**(2), 405-418.

Pokhrel, Y. N.; Fan, Y.; Miguez-Macho, G.; Yeh, P. J.-F. & Han, S.-C. (2013), 'The Role of Groundwater in the Amazon Water Cycle: 3. Influence on Terrestrial Water Storage and Comparison with GRACE', *Journal of Geophysical Research* **118**(8), 3233-3244.

Richardson, A. D.; Black, T. A.; Ciais, P.; Delbart, N.; Friedl, M. A.; Gobron, N.; Hollinger, D. Y.; Kutsch, W. L.; Longdoz, B.; Luysaert, S.; Migliavacca, M.; Montagnani, L.; Munger, J. W.; Moors, E.; Piao, S.; Rebmann, C.; Reichstein, M.; Saigusa, N.; Tomelleri, E.; Vargas, R. & Varlagin, A. (2010), 'Influence of spring and autumn phenological transitions on forest ecosystem productivity', *Philosophical Transactions of the Royal Society B: Biological Science* **365**, 3227-3246.

Richardson, A. D.; Baswell, B. H.; Hollinger, D. Y.; Jenkins, J. P. & Ollinger, A. V. (2009), 'Near-surface remote sensing of spatial and temporal variation in canopy phenology', *Ecological Applications* **19**(6), 1417-1428.

Richardson, A. D.; Keenan, T. F.; Migliavacca, M.; Ryu, Y.; Sonnentag, O. & Toomey, M. (2013), 'Climate change, phenology, and phenological control of vegetation feedbacks to the climate system', *Agricultural and Forest Meteorology* **169**, 156-173.

Rodell, M.; Chao, B. F.; Au, A. Y.; Kimball, J. S. & McDonald, K. C. (2005), 'Global Biomass Variation and Its Geodynamic Effects: 1982-98', *Earth Interactions*, **9**, 1-19.

Rodell, M. & Famiglietti, J. (2002), 'The potential for satellite-based monitoring of groundwater storage changes using GRACE: the High Plains aquifer, Central US', *Journal of Hydrology* **263**(1-4), 245-256.

Rodriguez-Iturbe, I. & Porporato, A. (2004), *Ecohydrology of Water-Controlled Ecosystems*:

Soil Moisture And Plant Dynamics, Cambridge University Press, Cambridge, UK.

[Rohr, T.; Manzoni, S.; Feng, X.; Menezes, R. S. C. & Porporato, A. \(2013\), 'Effect of rainfall seasonality on carbon storage in tropical dry ecosystems', *Journal of Geophysical Research* **118**, 1-12.](#)

[Roupsard, O.; Ferhi, A.; Granier, A.; Pallo, F.; Depommier, D.; Mallet, B.; Joly, H. I. & Dreyer, E. \(1999\), 'Reverse Phenology and Dry-Season Water Uptake by *Faidherbia albida* \(Del.\) A. Chev. in an Agroforestry Parkland of Sudanese West Africa', *Functional Ecology* **13**\(4\), 460-472.](#)

[Sankaran, M.; Hanan, N. P.; Scholes, R. J.; Ratnam, J.; Augustine, D. J.; Cade, B. S.; Gignoux, J.; Higgins, S. I.; Roux, X. L.; Ludwig, F.; Ardo, J.; Banyikwa, F.; Bronn, A.; Bucini, G.; Caylor, K. K.; Coughenour, M. B.; Diouf, A.; Ekaya, W.; Feral, C. J.; February, E. C.; Frost, P. G. H.; Hiernaux, P.; Hrabar, H.; Metzger, K. L.; Prins, H. H. T.; Ringrose, S.; Sea, W.; Tews, J.; Worden, J. & Zambatis, N. \(2005\), 'Determinants of woody cover in African savannas', *Nature* **438**\(8\), 846-849.](#)

[Sarmiento, G. \(1984\). 'The ecology of neotropical savannas', Harvard University Press, Cambridge, MA, USA.](#)

[Scanlon, T. M.; Caylor, K. K.; Manfreda, S.; Levin, S. A. & Rodriguez-Iturbe, I. \(2005\), 'Dynamic response of grass cover to rainfall variability: implications for the function and persistence of savanna ecosystems', *Advances in Water Resources* **28**, 291-302.](#)

[van Schaik, C. P.; Terborgh, J. W. & Wright, S. J. \(1993\), 'The Phenology of Tropical Forests: Adaptive Significance and Consequences for Primary Consumers', *Annual Review of Ecology and Systematics* **24**, 353-377.](#)

[Scheiter, S. & Higgins, S. I. \(2009\), 'Impacts of climate change on the vegetation of Africa: an adaptive dynamic vegetation modelling approach', *Global Change Biology* **15**, 2224-2246.](#)

[Schenk, H. J. & Jackson, R. B. \(2002\), 'The Global Biogeography of Roots', *Ecological Monographs* **72**\(3\), 311-328.](#)

[Schimper, A.F.W. \(1903\). 'Plant geography on a physiological basis' Oxford, UK: Clarendon Press.](#)

[Scholes, R. J. & Archer, S. R. \(1997\), 'Tree-Grass Interactions in Savannas', *Annual Review of Ecology and Systematics* **28**, 517-544.](#)

[Seghier, J.; Carreau, J.; Boulain, N.; Rosnay, P. D.; Arjounin, M. & Timouk, F. \(2012\), 'Is water availability really the main environmental factor controlling the phenology of woody vegetation in the central Sahel?', *Plant Ecology* **213**, 861-870.](#)

Seghier, J.; Do, F. C.; Devineau, J.-L. & Fournier, A. (2012), 'Phenology of Woody Species Along the Climatic Gradient in West Tropical Africa', in "Phenology and Climate Change" edited by Xiaoyang Zhang, published by IntechOpen. doi: 10.5772/33729.

Seghier, J.; Floret, C. & Pontanier, R. (1995), 'Plant phenology in relation to water availability: herbaceous and woody species in the savannas of northern Cameroon', *Journal of Tropical Ecology* **11**, 237-254.

Sellers, P. J.; Berry, J. A.; Collatz, G. J.; Field, C. B. & Hall, E. G. (1992), 'Canopy Reflectance, Photosynthesis, and Transpiration. III. A Reanalysis Using Improved Leaf Models and a New Canopy Integration Scheme', *Remote Sensing of Environment* **42**, 187-216.

Sheffield, J.; Goteti, G. & Wood, E. F. (2006), 'Development of a 50-Year High-Resolution Global Dataset of Meteorological Forcings for Land Surface Modeling', *Journal of Climate* **19**, 3088-3111.

Sheffield, J. & Wood, E. F. (2007), 'Characteristics of global and regional drought, 1950–2000: Analysis of soil moisture data from off-line simulation of the terrestrial hydrologic cycle', *Journal of Geophysical Research* **112**, D17115.

Shongwe, M. E.; van Oldenborgh, G. J.; van den Hurk, B. J. J. M.; de Boer, B.; Coelho, C. A. S. & van Aalst, M. K. (2009), 'Projected Changes in Mean and Extreme Precipitation in Africa under Global Warming. Part I: Southern Africa', *Journal of Climate* **22**, 3819-3837.

Sitch, S.; Huntingford, C.; Gedney, N.; Levy, P. E.; Lomas, M.; Piao, S. L.; Betts, R.; Ciais, P.; Cox, P.; Friedlingstein, P.; Jones, C. D.; Prentice, I. C. & Woodward, F. I. (2008), 'Evaluation of the terrestrial carbon cycle, future plant geography and climate-carbon cycle feedbacks using five Dynamic Global Vegetation Models (DGVMs)', *Global Change Biology* **14**(9), 2015-2039.

Solano, R.; Didan, K.; Jacobson, A. & Huete, A. (2010), 'MODIS Vegetation Index User's Guide (Collection 5)'. http://vip.arizona.edu/documents/MODIS/MODIS_VI_UsersGuide_01_2012.pdf.

Staver, A. C.; Archibald, S. & Levin, S. A. (2011), 'The Global Extent and Determinants of Savanna and Forest as Alternative Biome States', *Science* **334**, 230-232.

Stokli, R.; Rutishauser, T.; Baker, I.; Liniger, M. A. & Denning, A. S. (2011), 'A global reanalysis of vegetation phenology', *Journal of Geophysical Research* **116**, G03020.

Strassberg, G.; Scanlon, B. R. & Chambers, D. (2009), 'Evaluation of groundwater storage monitoring with the GRACE satellite: Case study of the High Plains aquifer, central United States', *Water Resource Research* **45**, W05410.

Swenson, S. & Wahr, J. (2006), 'Post-processing removal of correlated errors in GRACE data', *Water Resources Research* **33**, L08402.

Tapley, B. D.; Bettadpur, S.; Ries, J. C.; Thompson, P. F. & Watkins, M. M. (2004), 'GRACE Measurements of Mass Variability in the Earth System', *Science* **305**, 503-505.

Tateishi, R. & Ebata, M. (2004), 'Analysis of phenological change patterns using 1982–2000 Advanced Very High Resolution Radiometer (AVHRR) data', *International Journal of Remote Sensing* **25**(12), 2287-2300.

Trenberth, K. E.; Dai, A.; Rasmussen, R. M. & Parsons, D. B. (2003), 'The Changing Character of Precipitation', *Bulletin of American Meteorological Society* **84**, 1205-1217.

Vermote, E. F.; Kotchenova, S. Y. & Ray, J. P. (2011), 'MODIS Surface Reflectance User's Guide', Technical report, MODIS Land Surface Reflectance Science Computing Facility. http://modis-sr.ltdri.org/products/MOD09_UserGuide_v1_3.pdf

Vrieling, A.; de Leeuw, J. & Said, M. Y. (2013), 'Length of Growing Period over Africa: Variability and Trends from 30 Years of NDVI Time Series', *Remote Sensing* **5**(2), 982-1000.

Wagner, W.; Lemoine, G. & Rott, H. (1999), 'A Method for Estimating Soil Moisture from ERS Scatterometer and Soil Data', *Remote Sensing of Environment* **70**, 191-207.

Wang, B. & LinHo (2002), 'Rainy Season of the Asian–Pacific Summer Monsoon', *Journal of Climate* **15**, 386-398.

Ward, D.; Wiegand, K. & Getzin, S. (2013), 'Walter's two-layer hypothesis revisited: back to the roots!', *Oecologia* **172**, 617-630.

Weltzin, J. F.; Loik, M. E.; Schwinning, S.; Williams, D. G.; Fay, P. A.; Haddad, B. M.; Harte, J.; Huxman, T. E.; Knapp, A. K.; Lin, G.; Pockman, W. T.; Shaw, M. R.; Small, E. E.; Smith, M. D.; Smith, S. D.; Tissue, D. T. & Zak, J. C. (2003), 'Assessing the Response of Terrestrial Ecosystems to Potential Changes in Precipitation', *BioScience* **53**(10), 941-952.

White, M.; De Beurs, K.; Didan, K.; Inouye, D. W.; Richardson, A. D.; Jensen, O.; O'Keefe, J.; Zhang, G.; Nemani, R. R.; Van Leeuwen, W. J. D.; Brown, J. F.; De Wit, A.; Schaepman, M.; Lin, X.; Dettinger, M.; Bailey, A. S.; Kimball, J.; Schwartz, M. D.; Baldocchi, D. D.; Lee, J. T. & Lauenroth, W. K. (2009), 'Intercomparison, interpretation, and assessment of spring phenology in North America estimated from remote sensing for 1982–2006', *Global Change Biology* **15**, 2335-2359.

Yeang, H.-Y. (2007), 'The sunshine-mediated trigger of synchronous flowering in the tropics: the rubber tree as a study model', *New Phytologist* **176**, 730-735.

Zhang, X.; Friedl, M. A.; Schaaf, C. B.; Strahler, A. H.; Hodges, J. C.; Gao, F.; Reed, B. C. & Huete, A. (2003), 'Monitoring vegetation phenology using MODIS', *Remote Sensing of Environment* **84**, 471-475.

Zhang, X.; Friedl, M. A.; Schaaf, C. B.; Strahler, A. H. & Liu, Z. (2005), 'Monitoring the response of vegetation phenology to precipitation in Africa by coupling MODIS and TRMM instruments', *Journal of Geophysical Research* **110**, D12103.

Zhou, L.; Tucker, C. J.; Kaufman, R.; Slayback, D.; Shabanov, N. V. & Myneni, R. B. (2001), 'Variations in northern vegetation activity inferred from satellite data of vegetation index during 1981 to 1999', *Journal of Geophysical Research* **106**, D17, 20,069-20,083.

Accepted Article

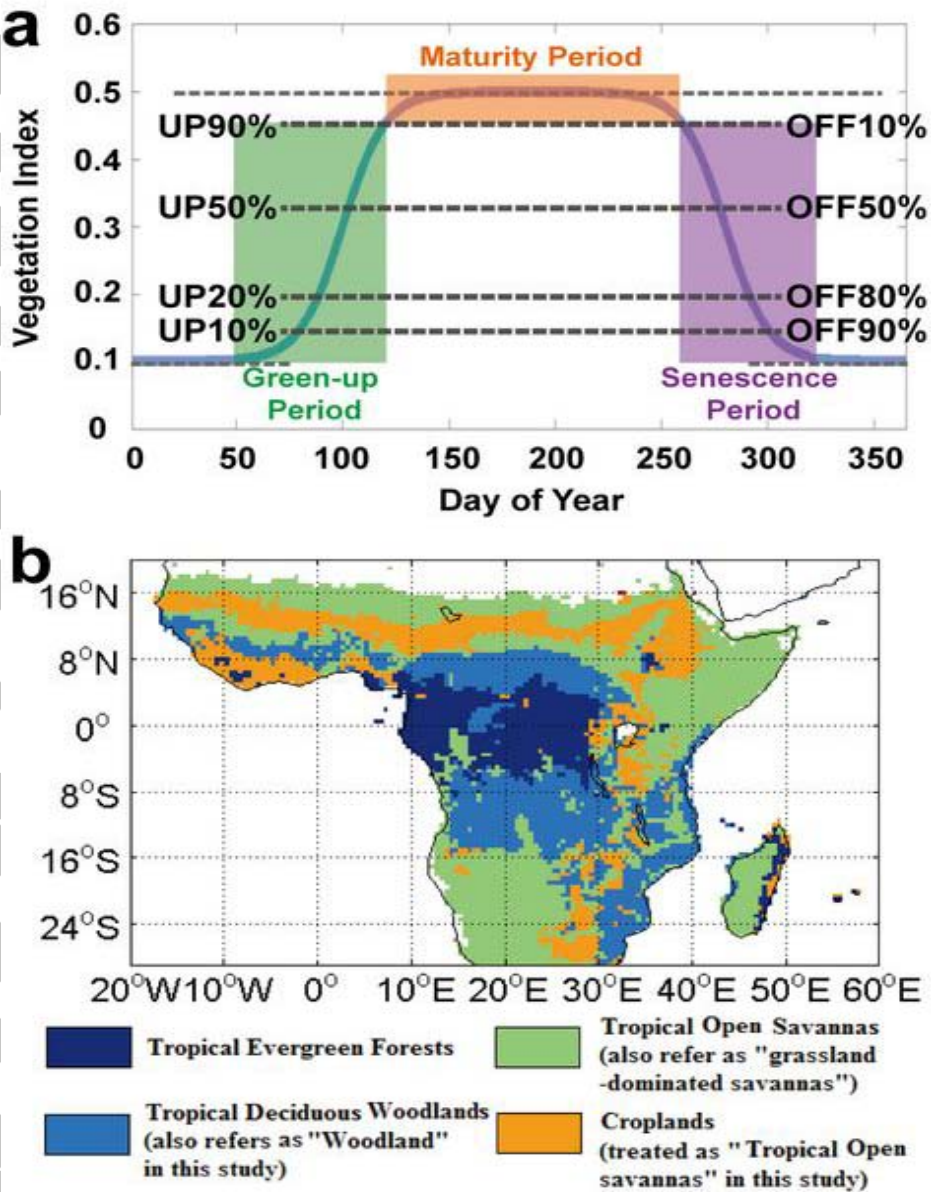


Figure 1. (a) Definition of Vegetation Index (VI) defined land surface phenological phases used in this investigation. (b) Simplified land cover map based on the GLC2000 Africa [Mayaux et al., 2003].

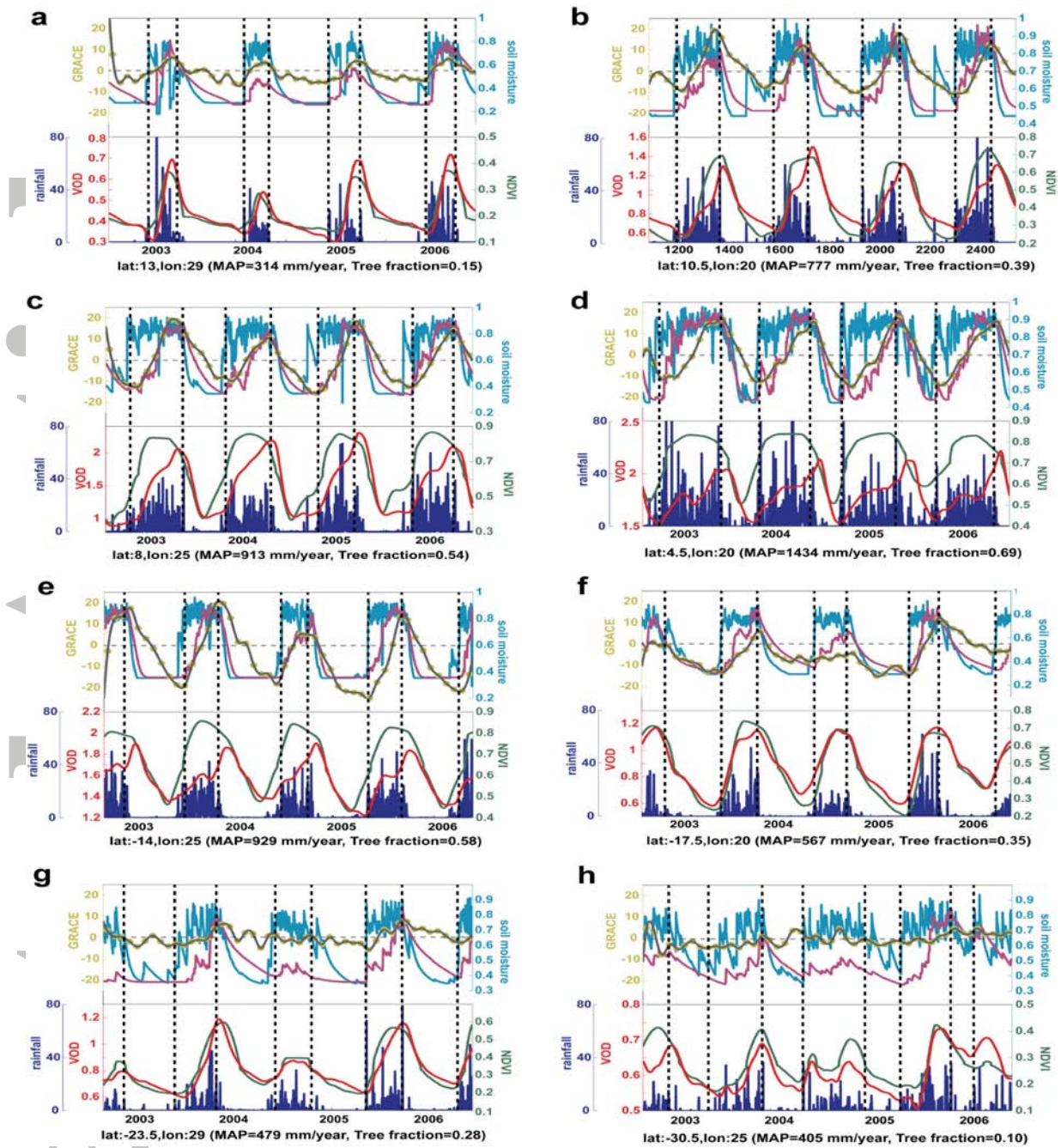


Figure 2. Time series of hydrological and vegetation variables for selected representative pixels across the African domain. Satellite derived variables include vegetation optical depth (VOD) from AMSR-E (red), GRACE derived terrestrial water storage (dark yellow), TRMM/TMI derived rainfall (blue bars), and MODIS derived NDVI (green); soil moisture at two-layers (0-10cm and 10cm-1m, blue and magenta respectively) is derived from a macroscale hydrological model (VIC). The corresponding locations of the selected pixels are in Figure 3c.

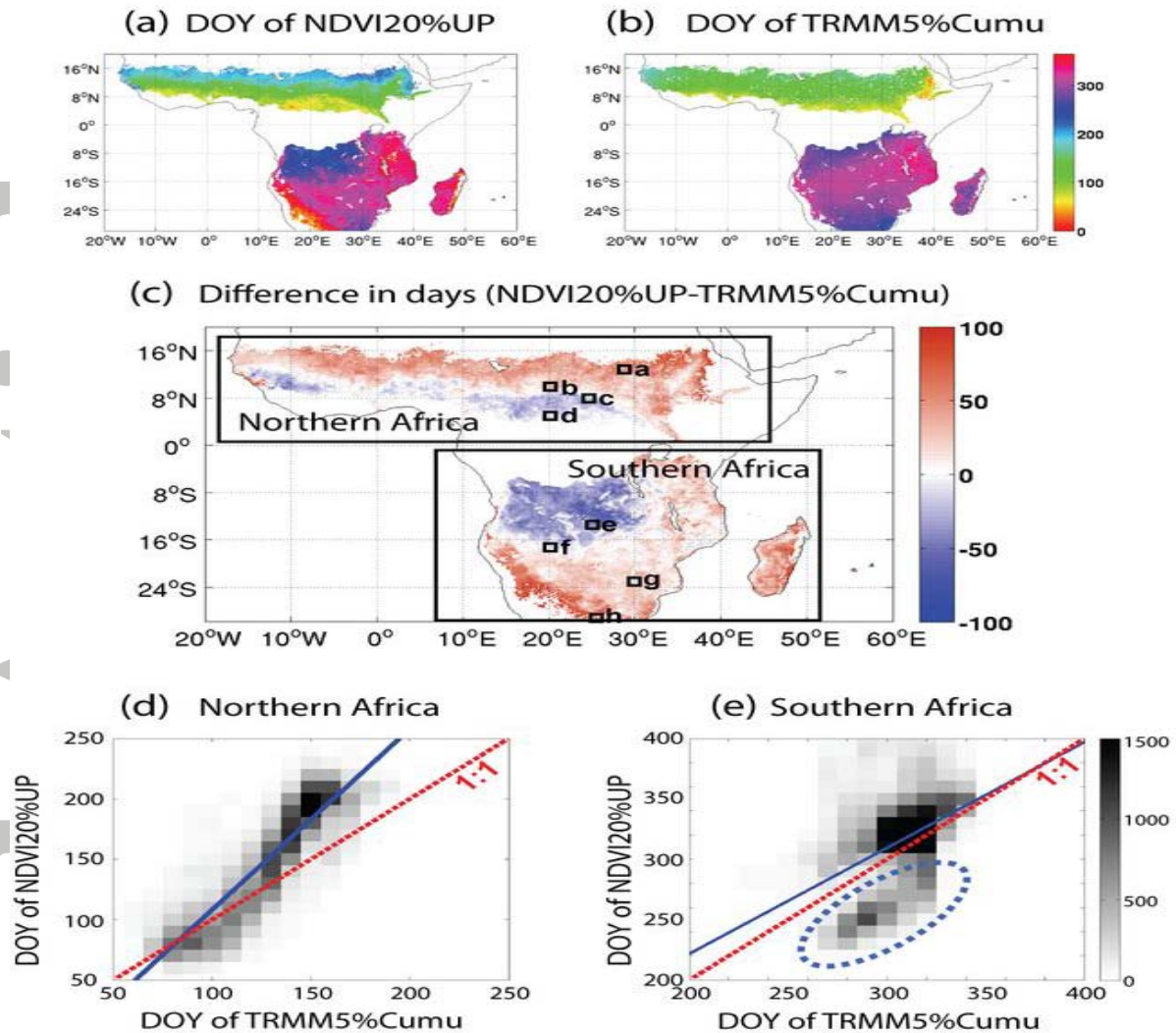


Figure 3. Relationship between satellite observed growing season and rainy season onset defined from respective MODIS NDVI and TRMM/TMI precipitation observations over African grassland and savanna; areas outside of the domain in (a), (b) and (c) are shown in white. (a) The growing season onset is defined here as the day (DOY) when NDVI reaches 20% in its seasonal green-up phase, and (b) the rainy season onset is defined as the DOY when rainfall reaches 5% of the annual accumulation of climatological MAP; (c) shows the pixel-wise differences between the onset of growing season and rainy season, and the small black squares denote locations of representative pixels shown in Figure 2; (d) and (e) show the pixel scatter density plots between the two onset times for the northern Africa and southern Africa, whose regions have been delineated in (c), the blue line is the linear regression between the onsets of rainy season and growing season, and the red dashed line refers to the 1:1 line.

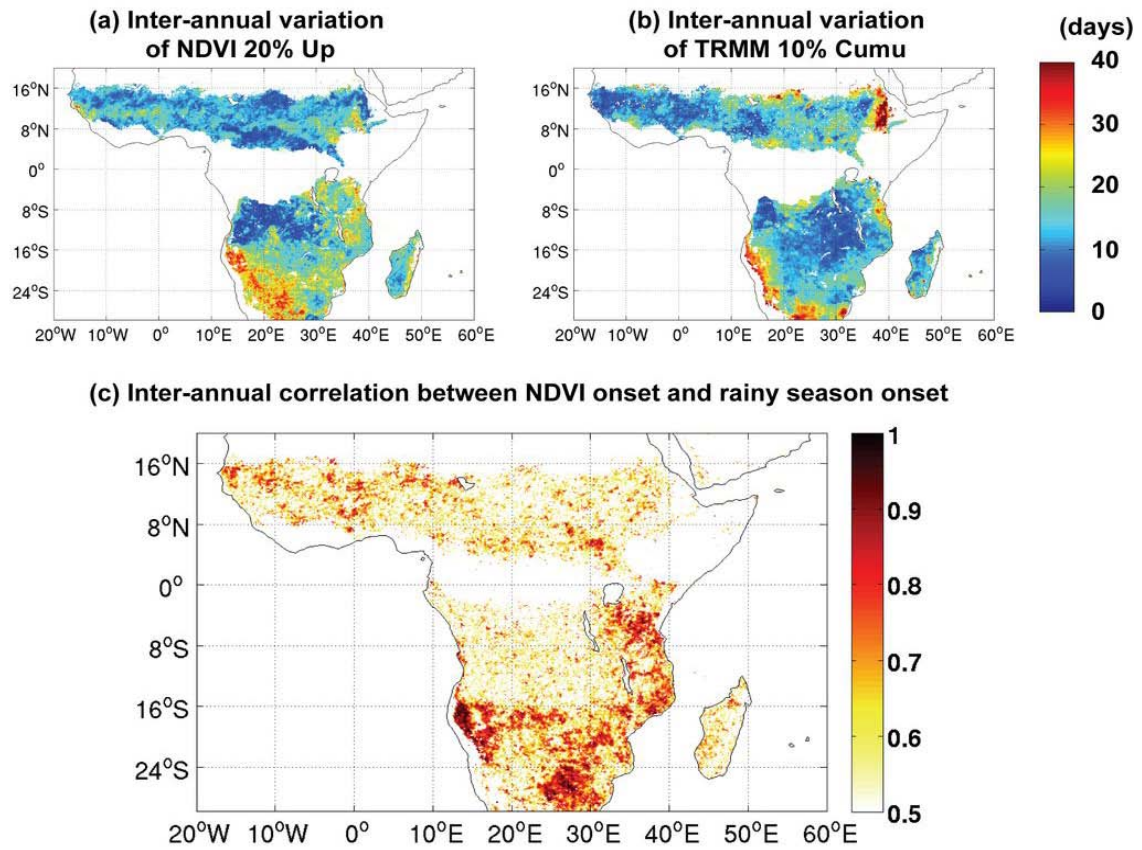
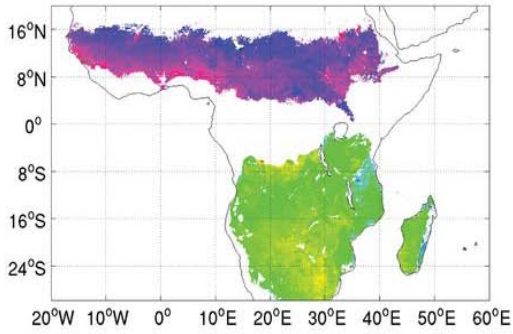
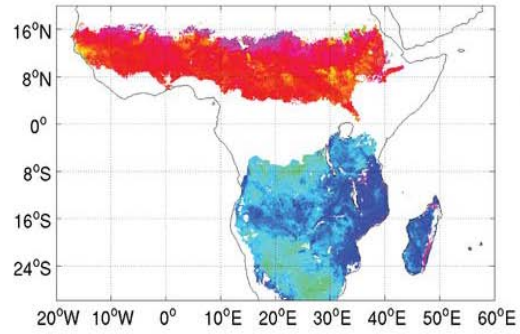


Figure 4. Inter-annual variability (standard deviation) and correlation between growing season and rainy season onsets defined from the MODIS NDVI and TRMM/TMI precipitation series over African grassland and savanna areas; areas outside of the domain are shown in white. (a) shows the inter-annual variation of growing season onset (inter-annual variation of NDVI20%UP). (b) shows the inter-annual variation of rainy season onset (the inter-annual variation of TRMM10%Cumulative). (c) shows the composited correlation between rainy season and growing season onsets (also see Figure S6).

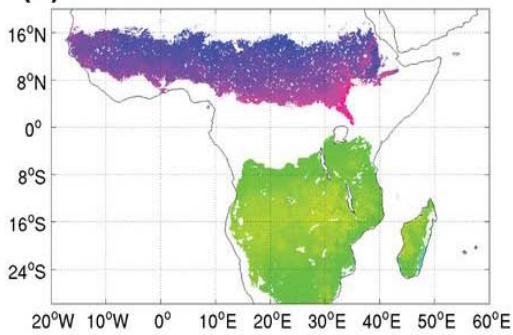
(a) DOY of NDVI 10% Off



(b) DOY of NDVI 90% Off



(c) DOY of TRMM 95% Cumu



(d) DOY of VOD Peak

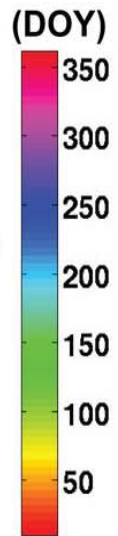
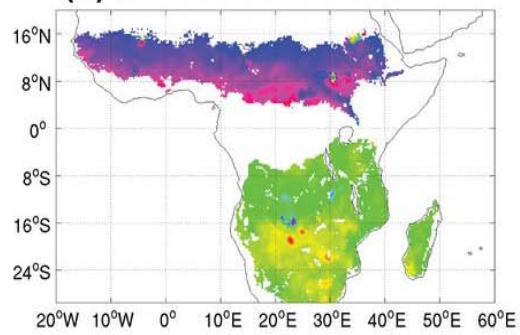


Figure 5. Satellite-data-derived senescence phases of vegetation and end of rainy season: (a) the DOY of NDVI 10% OFF from MODIS; (b) DOY of NDVI 90% OFF from MODIS; (c) DOY of TRMM 95% cumulative; (d) DOY of VOD peak.

Accepted

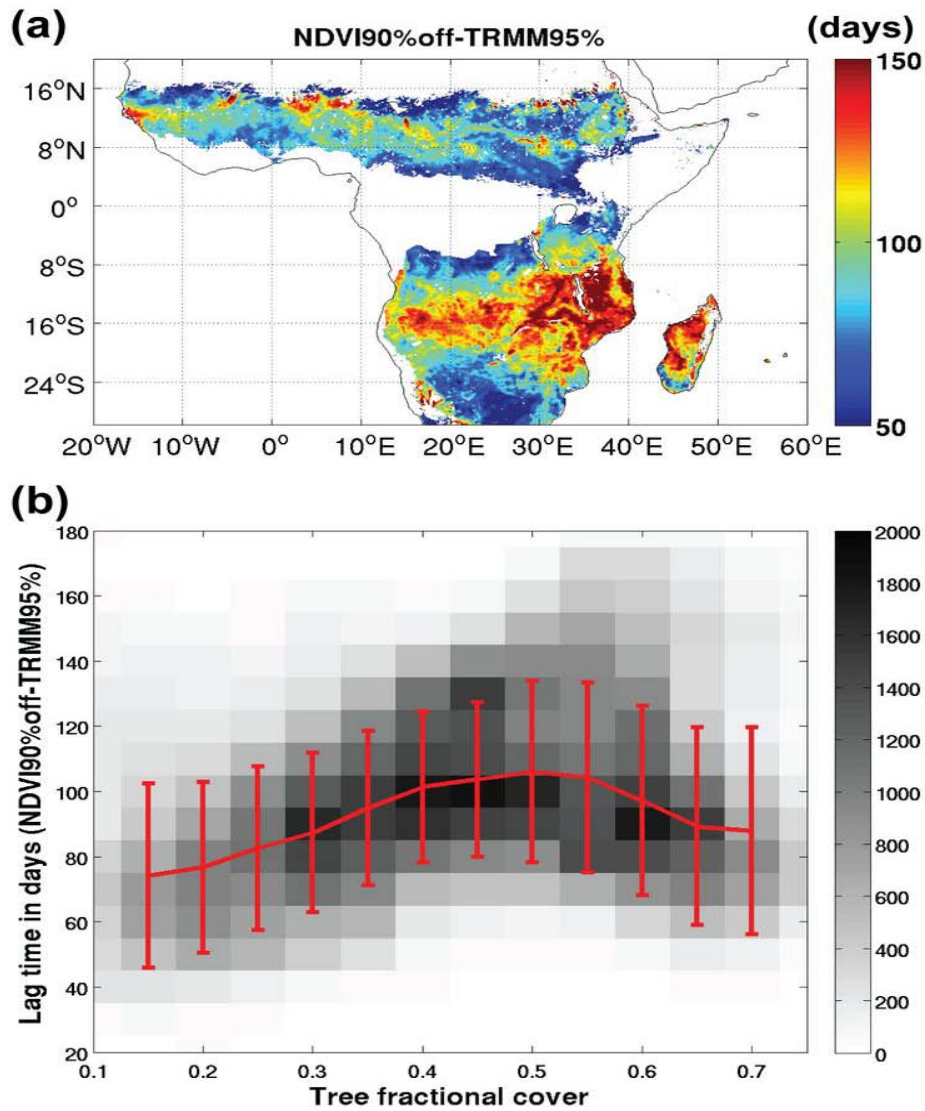


Figure 6. (a) Temporal lag (days) between vegetation full senescence (NDVI90%OFF) and the end of the rainy season (TRMM95%cumulative) determined from MODIS NDVI and TRMM precipitation, respectively, over the African domain. The corresponding relationship between tree fractional cover ([Guan et al., 2012](#)) and the lag time for all pixels in the domain is shown in (b).

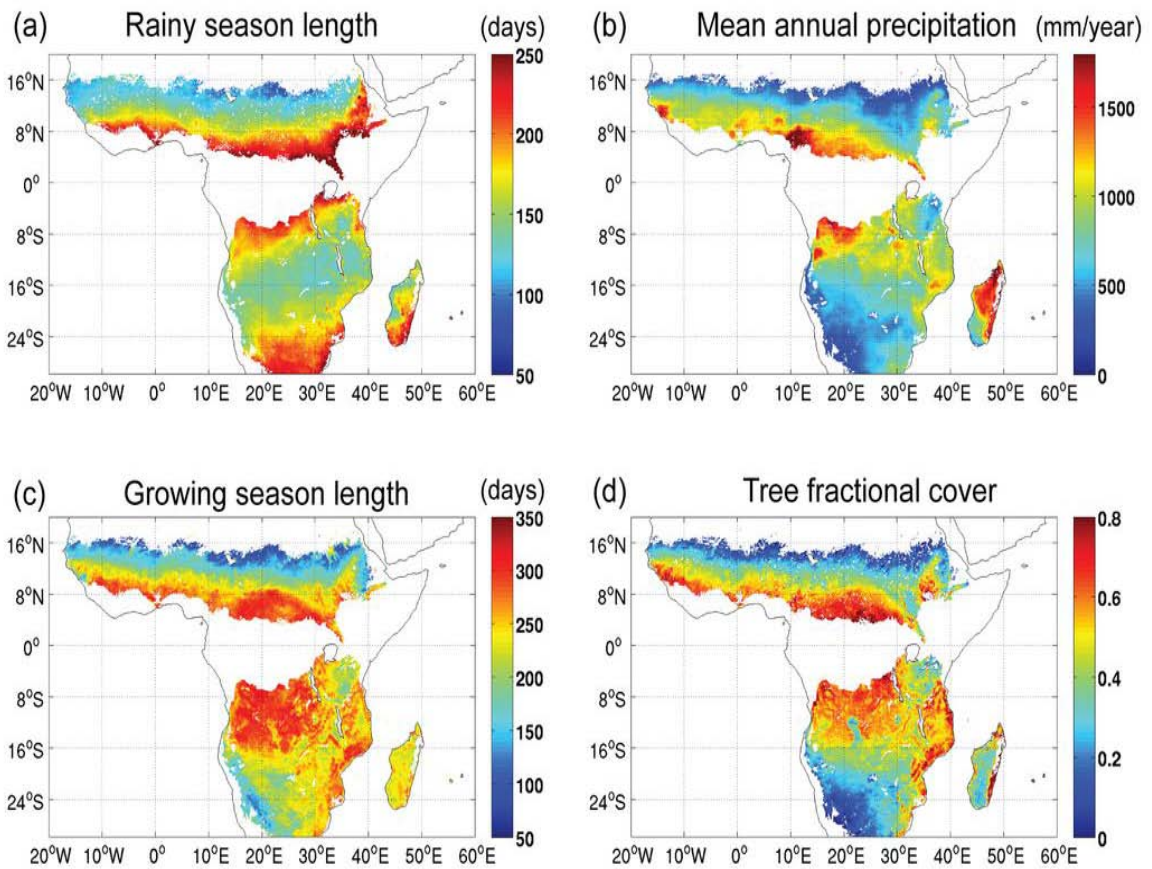


Figure 7. (a) Rainy season length (i.e. the difference between TRMM95%cumulative and TRMM5%cumulative); (b) mean annual precipitation; (c) growing season length (i.e. the difference between NDVI20%OFF and NDVI20%UP); (d) tree fractional cover (Guan et al., 2012).

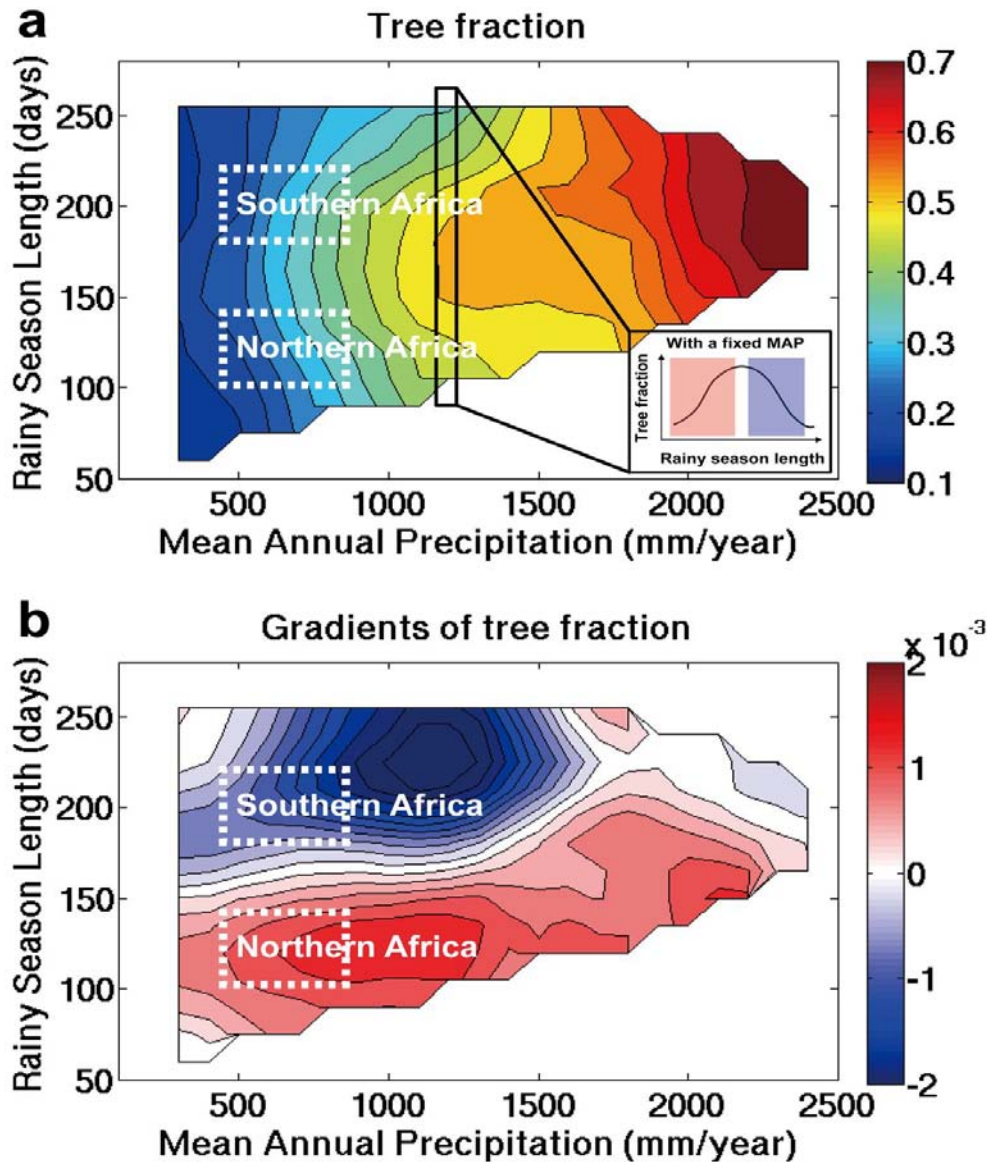


Figure 8. (a) Tree fraction as a function of both mean annual precipitation and rainy season length for the African domain. (b) Changes in tree fraction with rainy season length (%/day). Two dashed rectangular regions in both panels are correspondent to the two savanna regions shown in Figure S7. The inset in (a) presents a conceptual illustration of the nonlinear impacts of rainy season length on tree fraction cover at a fixed MAP, and the red and blue color shading refer to the positive and negative sensitivities, which are consistent with the colorshadings in (b).